Hindawi
Journal of Nanomaterials
Volume 2022, Article ID 3484613, 8 pages
https://doi.org/10.1155/2022/3484613

Research Article

Study of Mechanical Performance of BN Grafted Graphene Oxide Hybrid Aerogel for Polypropylene Composites

P. Nishanth,[1] G. Vimala,[2] L. Girisha,[3] M. Mahaveer Sree Jayan,[4] K. Balamanikandasuthan,[5] A. S. Rajesh,[6] V. K. Girish,[7] R. Thandaiah Prabu,[8] and Endalkachew Mergia Anbese[9]

[1]*Department of Aeronautical Engineering, East West College of Engineering, Bengaluru, Karnataka 560064, India*
[2]*Department of Chemistry, Chellammal Women's College, Guindy, Chennai, Tamil Nadu 600032, India*
[3]*Department of Mechanical Engineering, PES Institute of Technology and Management, Shivamogga, Karnataka 577205, India*
[4]*Department of Mathematics, Indra Ganesan College of Engineering, Tiruchirappalli, Tamil Nadu 620012, India*
[5]*Department of Mechanical Engineering, Velammal Institute of Technology, Chennai, 601204 Tamil Nadu, India*
[6]*Department of Mechanical Engineering, JSS Science & Technology University, Mysuru, Karnataka 570006, India*
[7]*Department of Mechanical Engineering, Panimalar Polytechnic College, Chennai, Tamilnadu, India*
[8]*Department of Electronics and Communication Engineering, Saveetha School of Engineering, SIMATS, -602105, Chennai, Tamilnadu, India*
[9]*Department of Civil Engineering, Ambo University, Ambo, Ethiopia*

Correspondence should be addressed to Endalkachew Mergia Anbese; endalkachew.mergia@ambou.edu.et

Received 16 March 2022; Accepted 3 May 2022; Published 23 May 2022

Academic Editor: Palanivel Velmurugan

Boron nitride-strengthened polymer matrix composites based on 3-dimensional porous materials are a considerable problem to develop. GO-BN aerogel (GO-BN) has been generated using a unique method for manufacturing large-scale 3D BNs and graphene oxide (GO) aerogels. Propylene was then added to the aerogel and polymerized in situ to create GO–BN/PP nanocomposites. Afterwards, the outcomes show that BNs and GO-BN were successfully established and that the 3D outlines using GO-BN aerogel have outstanding mechanical properties. Around 1% of the nanocomposite was used in its construction. This aerogel's thermal conductivity was 0.135 W/mK, and its mechanical properties were greatly improved over those of pristine PP, with increases of 10.12 percent in tensile strength and 48.4 percent in flexural strength and 61.5 percent in compression strength. They may now be produced in big quantities using this simple preparation procedure.

1. Introduction

A variety of industries, such as aerospace, military, and national security, as well as some engineering materials, have explored and deployed nanocomposites for their low weight and excellent performance [1, 2]. Nanomaterial dispersion within the polymer matrix can be improved with the use of 3D GO aerogels, which allow BNs to scatter equally in the aerogel wall before filling the matrix with the appropriate polymer material [3–5]. In prior investigations, GO-BN aerogels were made by physically mixing scattered BNs with the GO. However, grafting BNs onto the surface of GO has only been studied in a few methodical ways [6, 7]. Because of this, it is critical to investigate how the GO aerogel's BN structure and state affect the nanocomposites properties [8].

For nanocomposites, the application of three dimensional aerogel-strengthened filler has substantially enhanced the rough distribution of fillers and effectually improved their behavior [9]. According to [10, 11], the mechanical characteristics of nanocomposites made from graphene aerogels and poly methyl methacrylate were much better than those made using the usual blending and dispersion

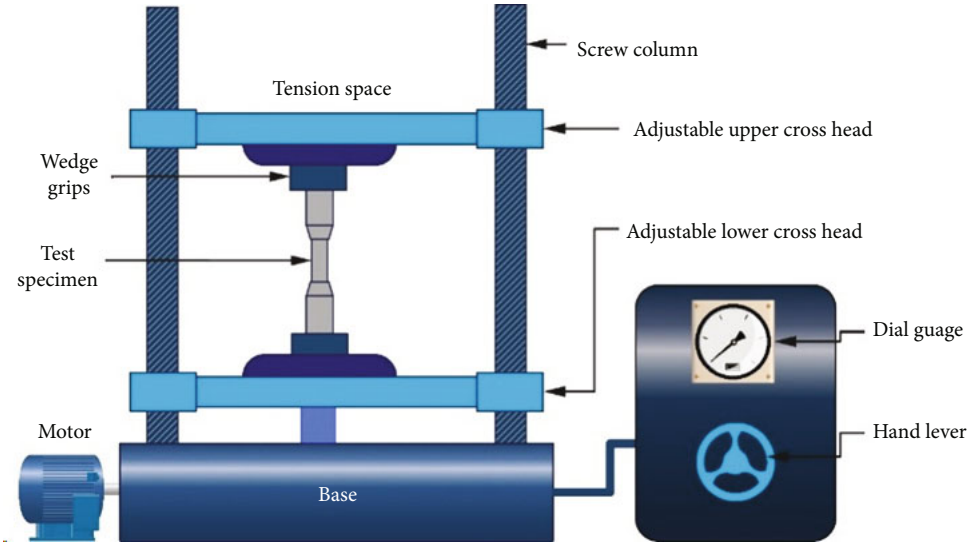

Figure 1: Universal testing machine.

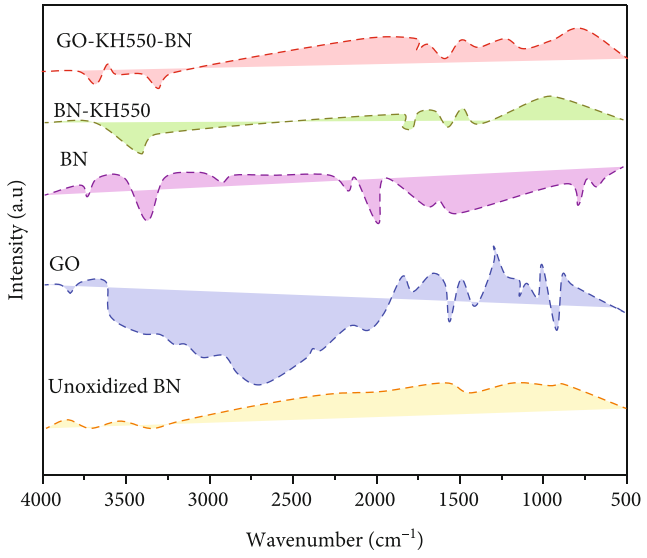

Figure 2: FTIR spectrum of GO, BN, BN-KH550, and GO-BN.

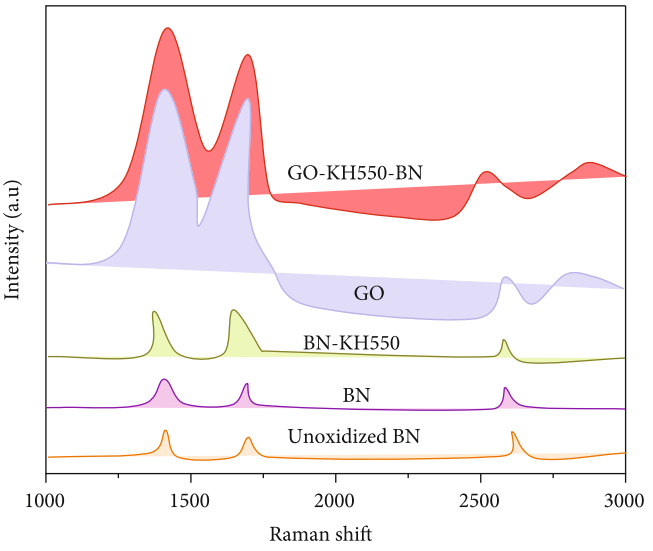

Figure 3: Raman spectroscopy.

process. Microhardness increased from 303.6 MPa to 462.5 MPa when graphene aerogel concentration was increased from 0.67 to 2.50 volume percent. Thermal conductivity was boosted by 1.44 times compared to epoxy resin, which had a 50% increase in mechanical strength and a 19.6% rise in elastic modulus [12, 13]. Nanocomposite hardness increased from 9.2 HV for graphene to 20.5 HV for aerogel-reinforced silicone rubber, a level greater than silicone rubbers, as a result of this process [14]. For dispersion in an epoxy matrix, [15] used a hybrid filler made from BNs grafted onto GO. Tensile modulus and strength both increased by 36% and 40%, according to the findings. There is no evidence that GO and BN designs have an impact on the characteristics of nanocomposites formed by physical mingling or chemical graft [16, 17]. To create large-scale aerogels, KH550 (3-aminopropyltriethoxysilane) was used to coat GO with BNs, then freeze drying was employed to create 3D structures. In situ polymerization of a propylene-initiator backfilled 3D aerogel produced the GO-BN/PP nanocomposites [18–21].

2. Experimental

2.1. Preparation of the GO-BN Aerogel. An enhanced Hummers' process was used to make GO out of graphite flakes. Sulfuric acid and nitric acid were used to oxidize BNs at

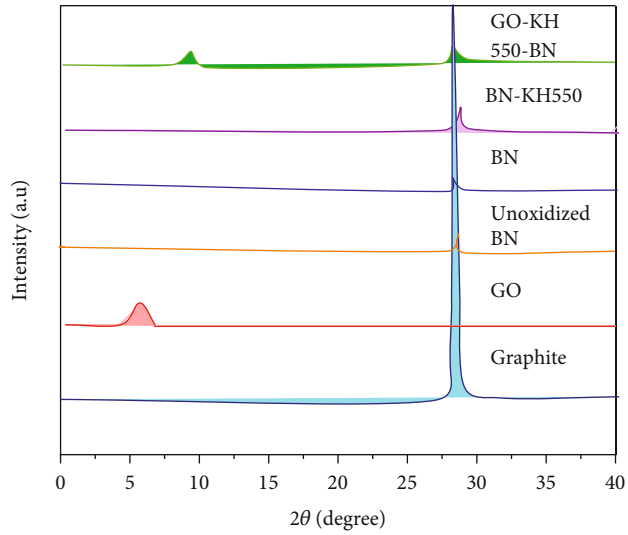

Figure 4: Boron nitride, GO, BN, BN-KH550, and BN-GO-BN XRD patterns.

100°C for eight hours, and the oxidized BNs were subsequently obtained through centrifugation, filtration, and freeze-drying. Sonication was used to mix the BNs (0.059 g) deionized water (21 mL) with ethanol (2 mL) for 1 hour. Sonication was used for three hours to break up the combination, which was then added to the GO suspension liquid (8.7 mL) (the mass proportion of BNs to GO was 3 : 7). Afterwards, the suspension was placed in an ice mold and frozen for 48 hours at a temperature of 25°C.

The GO-BN aerogel preparation was split into two stages. An ultrasonic dispersion of ethanol, water, and BN-KH550 in a three-necked flask was used to manufacture the modified BN-KH550. This was followed by 2 hours of ultrasonic dispersion, followed by 6 hours of stirring at 78°C. It was then freeze-dried to remove any remaining moisture from the combination [22]. A three-necked flask was used to mix GO with DI water and ethanol before ultrasonic dispersion took place for three hours to produce GO-BN. This mixture was then incubated for an additional two hours at room temperature with EDC/NHS (1 : 3). For the next 24 hours, a drop wise addition of the dispersed BN-KH550 solution was performed.

2.2. Preparation of GO-BN/PP Nanocomposites. Vacuum-assisted impregnation was used to completely replace the air in the GO-BN aerogel with a propylene/AIBN combination. Vacuum-assisted impregnation was used to immerse the created GO-BN aerogel in a propylene/AIBN mixture, which replaced the aerogel's air. Afterward, the complexes were kept at 75°C, 85°C, and 95°C for a total of 24 hours. Hot pressing at 6 MPa and 180°C for 5 minutes was used to eradicate antipores from the GO BN/PP nanocomposites [23]. During the hot-pressing technique, the nanocomposites were only compressed by 5%. The 7 : 3 weight-to-mass ratio of GO and BNs to a fresh PP matrix was used to synthesize GOC/PP nanocomposites.

2.3. Characterization. Infrared spectroscopy with a Fourier transform was utilized to examine the GO-BNs' morphology and chemical composition. Raman spectroscopy and X-ray diffraction were used apart for the plastic bending test [24]. An impact test at 7.5 J impact energy and a 32 mm sample length on the simple-supported beam impact tester were both done on the universal testing equipment in addition to the compression test at 5 mm/min. Figure 1 shows the universal testing machine.

3. Results and Discussion

3.1. Molecular Structure and Chemical Composition of GO, BN, BN-KH550, and GO-BN. FTIR was employed to evaluate the structures and compositions of the GO, BNs, BN-KH550, and GO-BN. Boron nitrides and graphene were found to have high concentrations of hydroxyl and carboxyl group PP in their absorption peaks at 3208 Hz and 1825 and 1156 Hz, respectively. BN-KH550 has an absorption peak of 1031 cm^{-1} due to the tensile vibration of the Si-O-C tensile vibration of KH550. There was a decrease in peak intensity at 3152 cm^{-1} for BN-KH550 grafted onto the surface of the GO. Figure 2 depicts the GO, BNs, BN-KH550, and GO-BN structures and compositions.

Graphene oxide, boron nitride, BN-KH550, and GO-BN Raman spectroscopy data are shown in Figure 3. Disorder on GO's surface and active group PP on BN's surface are both represented by solid bands at 1351 cm (the D band) and 1594 cm. There was an increase in ailment and responsiveness of BNs, BNs-KH550, and the ID/IG ratio of unoxidized (1.076), BNs (1.270), and BNs (1.466). As a result, BN-KH550 had a significant level of disorder and surface activity. Disruption and active group PP of GO and BN are more disordered than those of GO (1.705). For un oxidized boron nitrides (1.078), BNs (1.272), and BN-KH550 (1.468), the ID/IG ratio shows a progressive rise in disorder and reactivity.

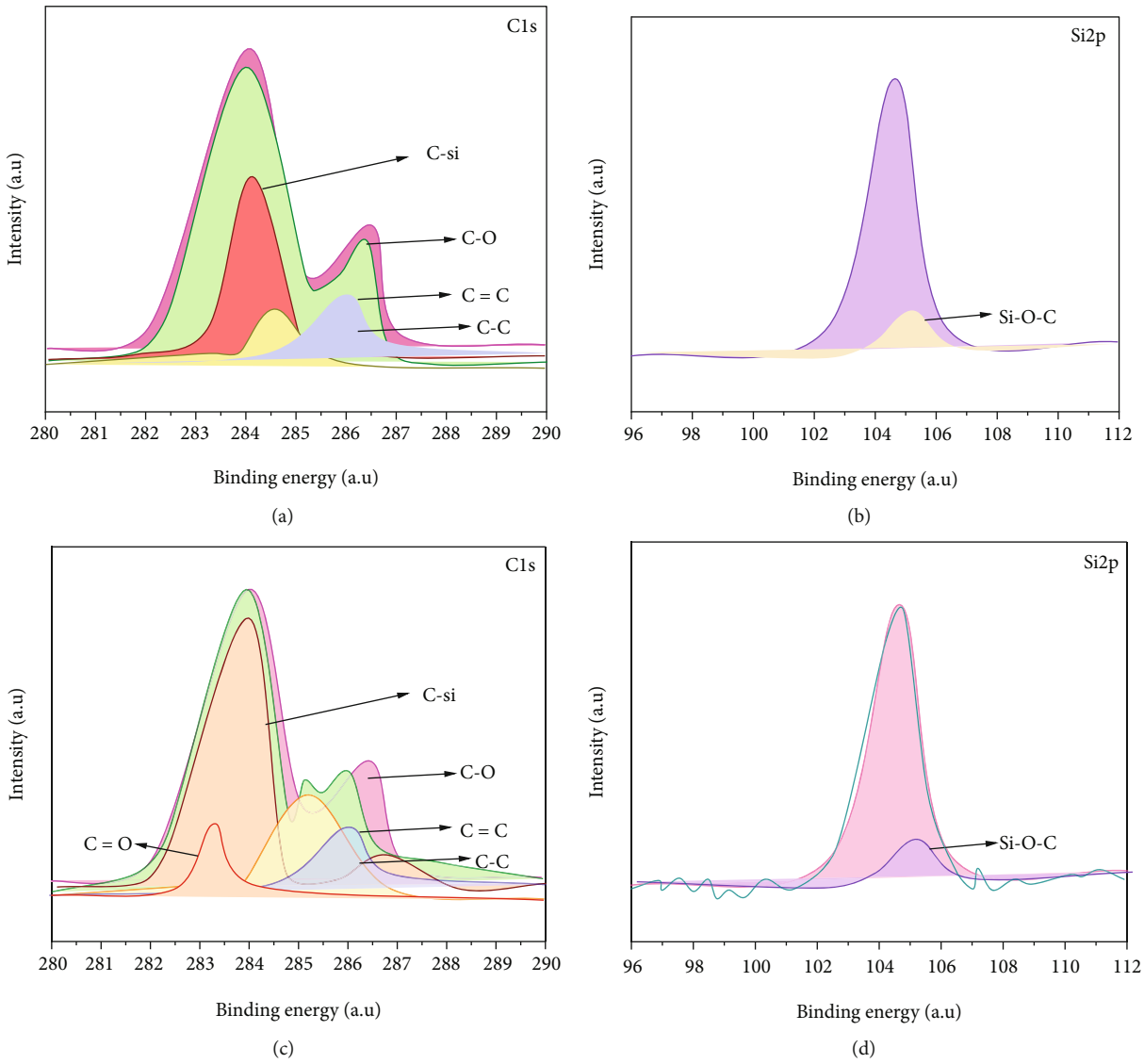

Figure 5: XPS spectra of graphene oxide, boron nitride, BN-KH550, and boron nitride-graphene oxide. (a) Cls spectrum of BN-KH550, (b) Si2p spectrum of BN-KH550, (c) Cls spectrum of GO-BN, and (d) Si2p spectrum of GO-BN.

Figure 4 shows that in graphene XRD patterns, a gap between the two layers of 0.34 nm and graphene oxide-BN structure is shown by the diffraction peak at 26.51. The presence of hydroxyl and carboxyl group PP in GO indicated that graphite had been successfully exfoliated during the chemical reaction. Hydroxyl and carboxyl group PP in BN-KH550 had no effect on interlayer distances, according to diffraction data taken at a temperature of 25.95° and unoxidized BNs. Interlayer spacing of GO-BN was lower (0.86 nm) than that of GO, suggesting reaction between those two materials.

As illustrated in Figure 5, surface chemical composition of GO, BNs, BN-KH550, and GO-BN was studied using XPP. BN-KH550 has been found to be grafted on top of both BNs and GO, as can be seen by comparing the peaks at 50 and 101 eV. On the graph in Figure 6, the binding energies of C-C (265.1 percent EV), C-O-C (266.2 eV), C=O (267.3 eV), and C-OH (265.2 eV) and C(C=O)-OH (268.4 eV) are all represented by six distinct peaks. These two BNs exhibit Si 2p regions with a specific binding energy of 1042 eV, as illustrated in Figure 6. There were several Si-O-C linkages on the GO surface after the BNs were grafted onto it.

It is shown in Figure 6 that the column aerogel has been compressed by 40% of its height in two sequential compressions. Next, in the first compression, it rebounded naturally with a compression strength of 0.28 MPa, and after two subsequent compressions, it maintained a strength of 0.09 MPa. This is because the GO and BNs are joined together to increase the aerogel, 45 percent of the aerogel's height. This is because the GO and BNs are connected together, which improves the aerogel's performance and reusability.

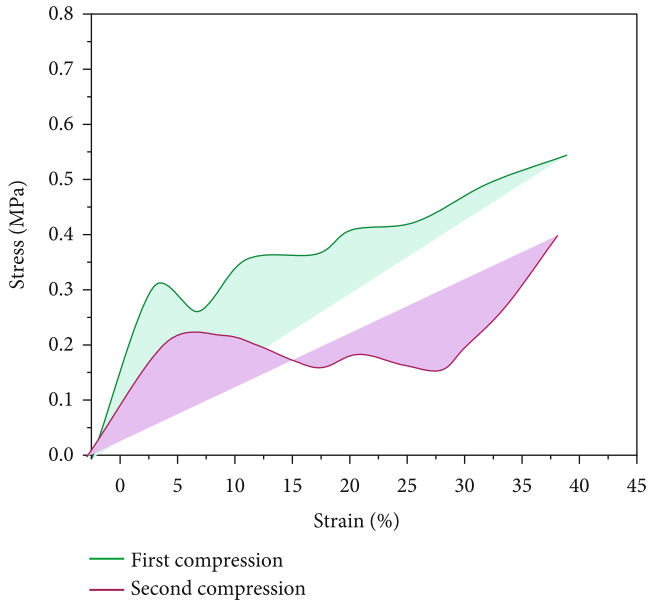

Figure 6: Compression stress-strain curves for GO-BN aerogels.

Table 1: Mechanical characteristics of different mixtures.

Sample	Tensile strength	Tensile strain	Flexural strength	Flexural strain	Impact strength	Compressive strength	Compressive strain
Polypropylene	8.45	0.815	19.5	0.89	1.92	34.6	8.4
GOC/PP	6.12	0.745	22.4	0.82	2.15	41.6	5.91
GO–BN/PP	9.56	1.426	28.5	1.86	2.224	54.5	11.36

3.2. Mechanical Properties of the Nanocomposites. GO-BN/P*P*values were 0.134 W/mK for PP (GO-BN/PP), GOC/PP, and PP-graphene oxide-boron nitride aerogel (GO-BN/PP). a 65 percent increase in heat conductivity over pure Poly Propylene (PP). Table 1 includes information on the qualities of the material's tensile and flexural strain, as well as its impact strength. If you compare pure PP to nanocomposites made with the GO-BN/PP nanomaterial, the tensile strength of the nanocomposites improved by 9.01 percent and their impact and compressive strengths by 46.88%. BN dispersion in GO aerogel and PP filling of aerogel pores directly influenced nanocomposites' mechanical characteristics. Figure 7 shows the mechanical characteristic of PP, GOC/PP, and GO-BN/PP.

Figure 8 shows that GO-BN/PP had an electrical conductivity of 0.158 ms/m and a thermal conductivity of 0.132 W/mK. Thermal conductivity increases by 60% over pure PP, which has no electrical conductivity. Because the BNs were linked and evenly disseminated, their superior electrical and thermal conductivity was increased. However, GO-BN/PP had lower electrical and thermal conductivity values than GOC/PP.

The following are some of the reasons for this:

(1) Damage to the 3D aerogel structure during hot pressing may result in inferior GO-BN/PP composite electrical and thermal conductivity qualities than the GOC/PP composite

(2) As a result, the thermal and electrical conductivities of GO-BN/PP composites were lesser than GOC/PP since a number of BNs between GO sheets were lowered. By doping GO sheets with BN, the composites' thermal and electric conductivity can be enhanced. When developing new composite materials, it is a model and inspiration

Also investigated were the thermal characteristics of the nanocomposite materials. Nanocomposite glass transition temperatures could not be improved since the 3D network structure for GO-BN was incomplete. GOCA/PP and GO-BN/PP composites also have a lower crystallisation temperature than pure polypropylene because of the GO's influence on polypropylene crystallisation, a comparison of the DSC curves for the various samples. For GO-BN/PP, physical cross linking in the entire GO-BN network in the nanocomposite was responsible for the greatest glass transition temperature. Although the GO-BN 3D network structure was not complete, the nanocomposites' glass transition temperature was not improved as a result. GOCA/PP and GO-BN/PP composites also have a lower crystallisation temperature than pure polypropylene because of the GO's influence on polypropylene crystallisation.

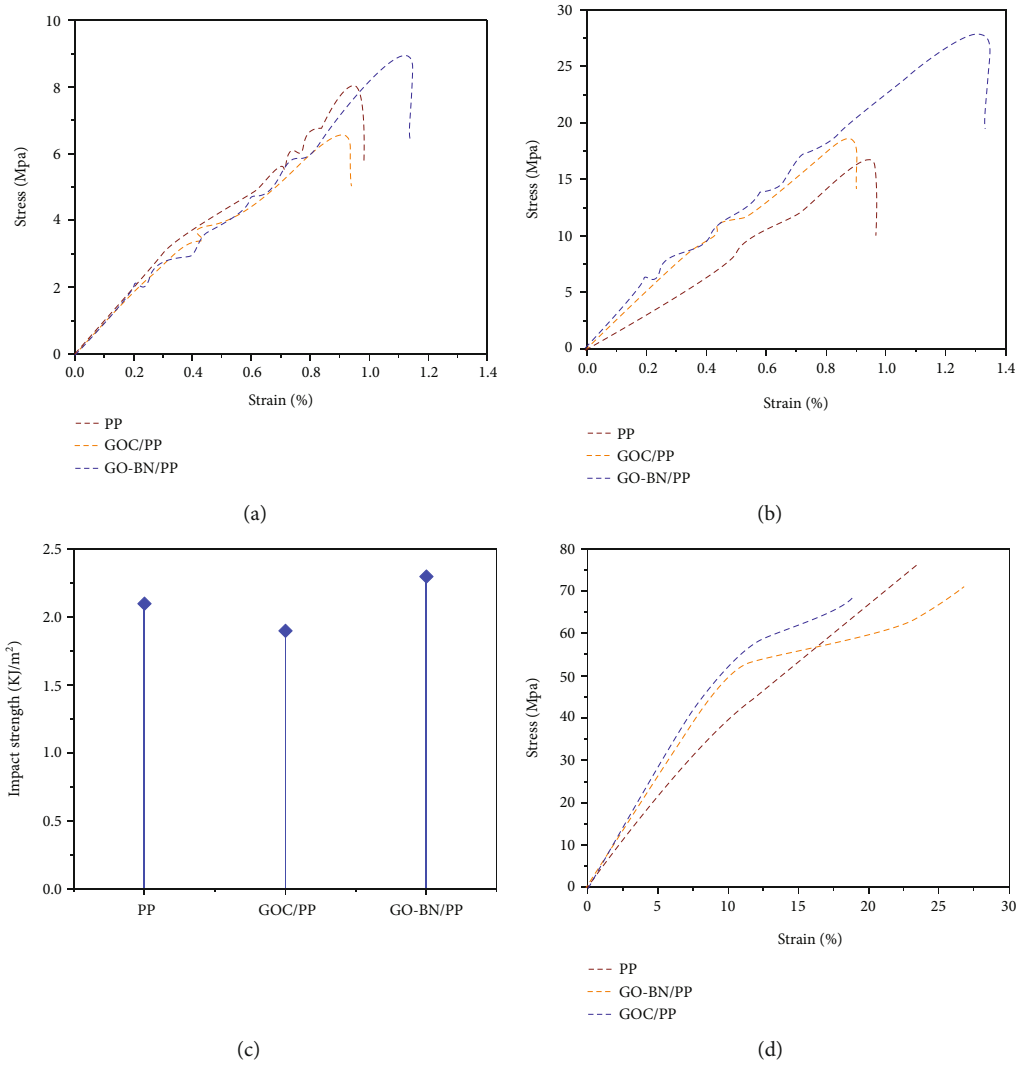

Figure 7: Mechanical characteristics of PP, GOC/PP, and GO-CNTA/PP. (a) emblematic stress-strain curves, (b) flexural stress-strain curves, (c) impact strength, and (d) compression curves of stress-strain.

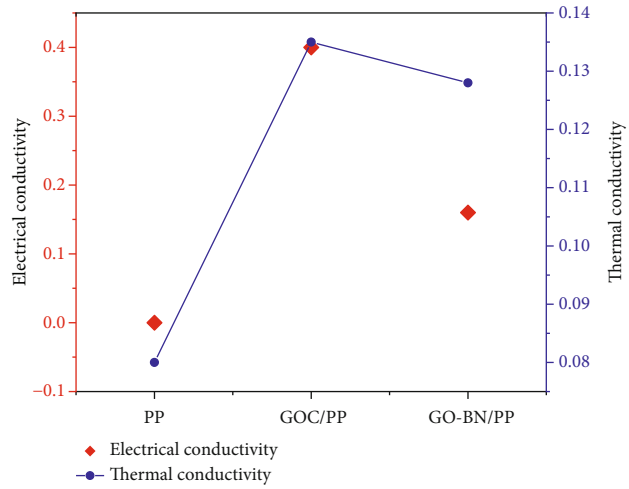

Figure 8: The thermal and electrical conductivity of neat PP, GOCA/PP, and GO-BN/PP.

4. Conclusions

Conventional splines appear to be tested quite infrequently in the fiction. This study established that a simple research strategy may be used to quickly produce large-scale nanocomposites of GO-BN aerogel and GO-BN/PP. Increased compatibility among inorganic components and polymers was achieved by modifying GO's surface energy and decreasing its surface tension. The compressive strength of the synthesized GO-BN/PP nanocomposites was found to be greater in the GO-BN/PP nanocomposites than in pure PP (tensile, flexural, impact, and compressive strength, respectively). When equated to pure PP, the GO-BN/PP nanocomposites had a thermal conductivity of 0.128 W/mK, which was 60 percent higher.

Data Availability

The data used to support the findings of this study are included within the article. Further data or information is available from the corresponding author upon request.

Conflicts of Interest

The authors declare that there is no conflict of interest regarding the publication of this article.

Acknowledgments

The authors appreciate the supports from Ambo University, Ambo, Ethiopia for the research and preparation of the manuscript. The authors appreciate the help from East West College of Engineering, PES Institute of Technology and Management, Indra Ganesan College of Engineering, JSS Science & Technology University, SIMATS, Chennai, for completing this work.

References

[1] M. L. Bharathi, S. Adarsh Rag, L. Chitra et al., "Investigation on wear characteristics of AZ91D/nanoalumina composites," *Journal of Nanomaterials*, vol. 2022, 9 pages, 2022.

[2] A. Chandrashekar, V. Mohanavel, A. R. Kaladgi et al., "The investigation of the effect of nano particles on dry sliding wear and corrosion behavior of Al-Mg/Al2O3 composites," *Surface Topography: Metrology and Properties*, vol. 9, no. 4, p. 045046, 2021.

[3] H. Xue, K. Chen, Q. Zhou, D. Pan, Y. Zhang, and Y. Shen, "Antimony selenide/graphene oxide composite for sensitive photoelectrochemical detection of DNA methyltransferase activity," *Journal of Materials Chemistry B*, vol. 7, no. 43, pp. 6789–6795, 2019.

[4] S. Ye, J. Feng, and P. Wu, "Highly elastic graphene oxide–epoxy composite aerogels via simple freeze-drying and subsequent routine curing," *Journal of Materials Chemistry A*, vol. 1, no. 10, pp. 3495–3502, 2013.

[5] W. Xiao, Y. Liu, and S. Guo, "Composites of graphene oxide and epoxy resin assuming a uniform 3D graphene oxide network structure," *RSC Advances*, vol. 6, no. 90, pp. 86904–86908, 2016.

[6] W. Zhang, Q. Q. Kong, Z. Tao et al., "3D thermally cross-linked graphene aerogel–enhanced silicone rubber elastomer as thermal interface material," *Advanced Materials Interfaces*, vol. 6, no. 12, p. 1900147, 2019.

[7] H. Hu, Z. Zhao, W. Wan, Y. Gogotsi, and J. Qiu, "Polymer/graphene hybrid aerogel with high compressibility, conductivity, and "sticky" superhydrophobicity," *ACS Applied Materials & Interfaces*, vol. 6, no. 5, pp. 3242–3249, 2014.

[8] S. Zhao, Y. Yan, A. Gao, S. Zhao, J. Cui, and G. Zhang, "Flexible polydimethylsilane nanocomposites enhanced with a three-dimensional graphene/carbon nanotube bicontinuous framework for high-performance electromagnetic interference shielding," *ACS Applied Materials & Interfaces*, vol. 10, no. 31, pp. 26723–26732, 2018.

[9] X. Liang and Q. Cheng, "Synergistic reinforcing effect from graphene and carbon nanotubes," *Composites Communications*, vol. 10, pp. 122–128, 2018.

[10] Y. Shang, T. Li, X. Zhu, Y. Zhang, X. Chen, and T. Zhao, "Effect of the graphene sheets derived from multistep oxidized carbon nanotubes on the performance of graphene sheets/poly (methyl methacrylate) composites," *Journal of Analytical and Applied Pyrolysis*, vol. 114, pp. 243–249, 2015.

[11] P. Hidalgo-Manrique, S. Yan, F. Lin et al., "Microstructure and mechanical behaviour of aluminium matrix composites reinforced with graphene oxide and carbon nanotubes," *Journal of Materials Science*, vol. 52, no. 23, pp. 13466–13477, 2017.

[12] Z. Fan, F. Gong, S. T. Nguyen, and H. M. Duong, "Advanced multifunctional graphene aerogel - poly (methyl methacrylate) composites: experiments and modeling," *Carbon*, vol. 81, pp. 396–404, 2015.

[13] Z. Chen, R. Wu, Y. Liu et al., "Ultrafine co nanoparticles encapsulated in carbon-nanotubes-grafted graphene sheets as advanced electrocatalysts for the hydrogen evolution reaction," *Advanced Materials*, vol. 30, no. 30, p. 1802011, 2018.

[14] Q. Cao, F. He, Y. Li et al., "Graphene-boron nitride hybrid aerogel/polyethylene glycol phase change composite for thermal management," *Fullerenes, Nanotubes and Carbon Nanostructures*, vol. 28, no. 8, pp. 656–662, 2020.

[15] Y. Li, L. Guo, Y. Wang, H. Li, and Q. Song, "A novel multiscale reinforcement by in-situ growing carbon nanotubes on graphene oxide grafted carbon fibers and its reinforced carbon/carbon composites with improved tensile properties," *Journal of Materials Science and Technology*, vol. 32, no. 5, pp. 419–424, 2016.

[16] W. Li, A. Dichiara, and J. Bai, "Carbon nanotube-graphene nanoplatelet hybrids as high-performance multifunctional reinforcements in epoxy composites," *Composites Science and Technology*, vol. 74, pp. 221–227, 2013.

[17] Y. Li, Z. Li, L. Lei et al., "Chemical vapor deposition-grown carbon nanotubes/graphene hybrids for electrochemical energy storage and conversion," *FlatChem*, vol. 15, p. 100091, 2019.

[18] N. Hsan, P. K. Dutta, S. Kumar, R. Bera, and N. Das, "Chitosan grafted graphene oxide aerogel: synthesis, characterization and carbon dioxide capture study," *International Journal of Biological Macromolecules*, vol. 125, pp. 300–306, 2019.

[19] H. Xu, X. Li, P. Li et al., "Enhancing mechanical performances of polystyrene composites via constructing carbon nanotube/graphene oxide aerogel and hot pressing," *Composites Science and Technology*, vol. 195, p. 108191, 2020.

[20] S. Kumar, M. Y. Wani, J. Koh, J. M. Gil, and A. J. F. N. Sobral, "Carbon dioxide adsorption and cycloaddition reaction of epoxides using chitosan-graphene oxide nanocomposite as a catalyst," *Journal of Environmental Sciences*, vol. 69, pp. 77–84, 2018.

[21] G. R. Bardajee, S. S. Hosseini, and C. Vancaeyzeele, "Graphene oxide nanocomposite hydrogel based on poly(acrylic acid) grafted onto salep: an adsorbent for the removal of noxious dyes from water," *New Journal of Chemistry*, vol. 43, no. 8, pp. 3572–3582, 2019.

[22] Y. Xie, W. Liu, C. Liu et al., "Investigation of covalently grafted polyacrylate chains onto graphene oxide for epoxy composites with reinforced mechanical performance," *Journal of Applied Polymer Science*, vol. 136, no. 32, p. 47842, 2019.

[23] H. Liu, X. Wang, C. Ding et al., "Carboxylated carbon nanotubes-graphene oxide aerogels as ultralight and renewable high performance adsorbents for efficient adsorption of glyphosate," *Environment and Chemistry*, vol. 17, no. 1, pp. 6–16, 2020.

[24] E. Wang, Y. Dong, M. D. Z. Islam et al., "Effect of graphene oxide-carbon nanotube hybrid filler on the mechanical property and thermal response speed of shape memory epoxy composites," *Composites Science and Technology*, vol. 169, pp. 209–216, 2019.